# Construction of miRNA-mRNA regulatory network and prognostic signature in endometrial cancer

**Jinhui Liu**
Department of Gynecology, The First Affiliated Hospital of Nanjing Medical University
**Rui Sun**
Department of Gynecology, The First Affiliated Hospital of Nanjing Medical University
**Sipei Nie**
Department of Gynecology, The First Affiliated Hospital of Nanjing Medical University
**Jing Yang**
Department of Gynecology, The First Affiliated Hospital of Nanjing Medical University
**Siyue Li**
Department of Gynecology, The First Affiliated Hospital of Nanjing Medical University
**Yi Jiang**
Department of Gynecology, The First Affiliated Hospital of Nanjing Medical University
**wenjun Cheng** ( wenjunchengdoc@163.com )
Department of Gynecology, The First Affiliated Hospital of Nanjing Medical University, Nanjing

**Research**

**Keywords:** TCGA, endometrial cancer, miRNA-mRNA network, prognostic model, immune infiltration cell

**Posted Date:** February 18th, 2020

**DOI:** https://doi.org/10.21203/rs.2.23832/v1

# Construction of miRNA-mRNA regulatory network and prognostic signature in endometrial cancer

Jinhui Liu[1†], Rui Sun[1†], Sipei Nie[1†], Jing Yang[1], Siyue Li[1], Yi Jiang[1], Wenjun Cheng[1*]

*Correspondence: wenjunchengdoc@163.com

†Jinhui Liu, Rui Sun and Sipei Nie contributed equally to this work.

[1] Department of Gynecology, The First Affiliated Hospital of Nanjing Medical University, Nanjing 210029, Jiangsu, China.

## Abstract

**Background:** Many studies have well supported the close relationship between miRNA and endometrial cancer (EC). This bioinformatic study, compared with other similar studies, confirmed a new miRNA-mRNA regulatory network to investigate the miRNA-mRNA regulatory network and the prognostic biomarkers in EC.

**Methods:** We downloaded RNA-seq and miRNA-seq data of endometrial cancer from the TCGA database, and then we used EdegR package to screen differentially expressed miRNAs and mRNAs (DE-miRNAs and DE-mRNAs). The differentially expressed genes (DEGs) were identified and their functions were predicted using the functional and pathway enrichment analysis. Protein–protein interaction (PPI) network was established using STRING database, and the hub genes were verified by Gene Expression Profiling Interactive Analysis (GEPIA). Then, we constructed a

regulatory network of EC-associated miRNAs and hub genes by Cytoscape, and determined the expression of unexplored miRNAs in EC tissues and normal adjacent tissues by quantitative Real-Time PCR (qRT-PCR). A prognostic signature model and a predictive nomogram were constructed. Finally, we explored the association between the prognostic model and the immune cell infiltration.

**Results:** 11531 DE-mRNAs and 236 DE-miRNAs, as well as 275 and 118 candidate DEGs for upregulated and downregulated DE-miRNAs were screened out. These DEGs were significantly concentrated in FOXO signaling pathway, cell cycle and Focal adhesion. Among the 20 hub genes identified, 17 exhibited significantly different expression compared with normal tissues. The miRNA-mRNA network included 5 downregulated and 13 upregulated DE-miRNAs. qRT-PCR proved that the expression levels of miRNA-18a-5p, miRNA-18b-5p, miRNA-449c-5p and miRNA-1224-5p and their target genes, NR3C1, CTGF, MYC, and TNS1 were consistent with our predictions. Univariate and multivariate Cox proportional hazards regression analyses of the hub genes revealed that NR3C1, EZH2, and GATA4 showed a significant prognostic value. We identified the three-gene signature as an independent prognostic indicator for EC ($p$=0.022，HR=1.321, 95% CI: 1.041-1.675) and these genes were closely related to eight types of immune infiltration cells.

**Conclusion:** Our study revealed the mechanisms of the carcinogenesis and progression of EC.

**Keywords:** TCGA, endometrial cancer, miRNA-mRNA network, prognostic model, immune infiltration cell.

## Introduction

Endometrial cancer (EC), a common malignancy, has an estimated incidence of 10–20 per 100,000 women globally and the figure is still increasing [1]. Surgical treatment is the major therapy for early stage EC patients [2]. The prognosis of advanced EC is poor, with a 5-year overall survival rate of 15–17% [3]. Identifying effective targets for EC tumorigenesis and treatment would be beneficial to the survival of EC patients.

MicroRNAs (miRNAs), the 19-25 nucleotide non-coding RNAs, regulate gene expression and participate in biological processes[4]. By base-pairing with complementary sequences within messenger RNA (mRNA) molecules, miRNA can silence RNAs and regulate post-transcriptional gene expression to promote cell proliferation[5], apoptosis[6], cell cycle[7], migration[8], differentiation[9], and energy metabolism[10]. The dysregulation of miRNA is linked to multiple diseases, like obesity, cancer, cardiovascular diseases, inflammatory diseases and disorders of the female reproductive system[11-16]. Many studies have well supported the close relationship between miRNA and EC[17]. For example, the overexpressed miR-137 suppresses tumor cell proliferation and colony formation in vitro and xenograft tumor growth in vivo[18]. Despite the previous analyses on the miRNA expression in EC, this bioinformatic study, compared with other similar studies, confirmed a new miRNA-mRNA regulatory network.

In our study, the differentially expressed miRNAs (DE-miRNAs) in EC were screened using TCGA database (**Fig. 1**). The functions of the DE-miRNA target genes were predicted by the functional and pathway enrichment analysis. Then, the regulatory network of EC-associated miRNAs and their target genes was established, and the expression of unexplored EC-associated miRNAs was determined using qRT-PCR. Finally, we built a prognostic signature model using the hub genes and explored the association between the prognostic model and immune cell infiltration.

## Methods

### Study Population

The mRNAs expression profiles of 587 (552 EC and 35 normal) tissues, and the miRNA isoform expression profiles of 568 (546 EC and 22 normal) tissues from TCGA database (http://cancergenome.nih.gov/publications/publicationguidelines ) were downloaded with the corresponding clinical data collected. The sequenced data were downloaded from Illumina HiSeq RNASeq and Illumina HiSeq_miRNASeq platforms.

### Screening DE-mRNAs and DE-miRNAs

We used the "edegR" package operated by R software to screen out DE-mRNAs and DE-miRNAs. DE-miRNAs were defined as $|\log_2$ fold change (FC)$| > 2.0$ and adjusted $P < 0.01$. DE-mRNAs were identified if $|\log_2 FC| > 1.0$ and adjusted $P < 0.05$.

**Differentially expressed genes**

To get the downstream target genes of DE-miRNAs, we used miRTarBase (http://mirtarbase.mbc.nctu.edu.tw/php/index.php ), miRDB (http://www.mirdb.org/ ), and TargetScan (http://www.targetscan.org/ ) to determine whether the DE-miRNAs and the target genes were paired. The differentially expressed genes (DEGs) and the overlapping genes of DE-mRNAs and miRNA target genes were identified using Venn diagram (https://bioinfogp.cnb.csic.es/tools/venny/ ).

**Functional annotation and pathway enrichment analysis**

Gene Ontology (GO) analysis, the Kyoto Encyclopedia of Genes and Genomes (KEGG) pathway enrichment analysis were used to detect the functions of the target genes. The categories of GO functional annotation included biological process (BP), cellular component (CC), and molecular function (MF). The Enrichr database (http://amp.pharm.mssm.edu/Enrichr/ ) was applied in GO functional annotation and KEGG pathway enrichment analysis for the overlapping target genes and DE-mRNAs. $P < 0.05$ was used as the threshold.

**Construction of protein-protein interaction**

To reveal functional interactions and relationships between protein products of the DEGs in EC, we uploaded all the overlapping genes screened from the Search Tool for the Retrieval of Interacting Genes (STRING) database (http://string-db.org/ ). Subsequently, the hub genes in the network were identified according to the degree of

connectivity using Cytoscape software (version 3.6.1). We used “MCODE” plug-in to visualize and select modular hubs in the PPI network (degree = 4, node score = 0.2, k-core = 2, and max. depth = 100). The node in the network represented a gene or a protein and the line between the nodes represented their interaction. Central nodes represented key or significant proteins or genes with important functions. We recognize the top 10 hub nodes as hub genes.

**Validation of hub gene expression levels**

The validation of the expression levels of top 20 hub genes were conducted using the Gene Expression Profiling Interactive Analysis (GEPIA) [19]. Statistical difference was defined as hub genes with $|\log_2 FC| > 2$ and $p < 0.01$.

**Establishment of miRNA-mRNA regulatory pathways and corresponding transcription factors**

We built a miRNA-mRNA network to identify the most functional miRNAs and used the Cytoscape software (version 3.6.1) to establish the miRNA-hub gene network and then to investigate the association between the 20 hub genes and the DE-miRNAs. The selected upregulated and downregulated DE-miRNAs were input into FunRich software to predict the upstream transcription factors of screened DE-miRNAs.

**RNA Extraction and quantitative Real-Time PCR (qRT-PCR)**

Total RNA of 42 (21 pairs of tumor and paired paratumor) tissues was separated using

Trizol reagent (Thermo Fisher Scientific, Waltham, MA). The RNA quantity control and concentration was evaluated using NanoDrop 2000 Spectrophotometer (Thermo Scientific, Wilmington, DE, USA). The reverse transcription of total RNA was performed using the Reverse Transcription Kit (Takara, Tokyo, Japan). qRT-PCR were conducted (SYBR Premix Ex Taq, TaKaRa, Dalian, China) on Light Cycler 480 (Roche, Switzerland) to detect the relative miRNA and mRNA expressions using the $2^{-\Delta\Delta Ct}$ method, in which GAPDH and U6 were used as endogenous control for mRNA and miRNA, respectively. The PCR primers are listed in **Supplemental Table 1**.

**Establishment of prognostic signature model using hub genes**

The association between the hub gene expression and the overall survival was assessed using the univariate Cox proportional hazards regression analysis. Then, the prognosis-related genes ($p$<0.05) were taken as candidate variables, and stepwise multivariate Cox proportional hazards regression analysis was employed to predict the risk score of the genes. The model was developed using the coxph() function in survival package[20]. The risk score for predicting the overall survival was calculated as follows: Risk score = exp RNA1 * β RNA1 + exp RNA2 * β RNA2 + exp RNA3 * β RNA3 + …exp RNAn * β RNAn (exp RNA: relative expression value after transforming z score; β RNA: regression coefficient obtained via the multivariate Cox proportional hazards regression model). The patients fell into a low-risk group and a high-risk group based on the mean risk score. We used the “survival” package in R to generate the overall survival curves of both groups. The 1-, 3-, and 5-year receiver

operating characteristic (ROC) curves were used to calculate the predictive value of the model. The sensitivity and specificity of the risk model of EC were calculated by the ROC curve using the "survival ROC" R package. The areas under the ROC curve (AUC) presenting sensitive and specific cities were used to indicate the predictive value. The predictive model, established with the AUC >0.6, was considered to have explanatory and informative efficacy. In addition, comprehensive survival analysis was implemented to analyze the relationship between the different clinical parameters (age, race, tumor stage, histological type, grade, and tumor status) and the risk score model. Clinical based subgroup survival analysis stratified by clinical factors was also conducted. All analyses were conducted using the R. $P < 0.05$ was considered statistically significant in the prognostic signature analysis. Finally, we built and validated a predictive nomogram[21]. Clinical parameters like age, race, tumor stage, histological type, grade, and tumor status, and the risk score model, were used to build a nomogram to investigate the probability of 1-, 3-, and 5-OS of EC. Validity of the nomogram was assessed by discrimination and calibration.

**Association of prognostic signature with immune cells infiltration**

To investigate the prognostic signature, CIBERSORT was used to search the most significant tumor-infiltrating immune cells and prognostic signature of the risk score[22]. We explored the relationship between the risk score and the significant immune cells, including B cells memory fraction, B cells naive fraction, dendritic cells activated fraction, dendritic cells resting fraction, eosinophils fraction,

macrophages M0 fraction, macrophages M1 fraction, macrophages M2 fraction, mast cells resting fraction, monocytes fraction, neutrophils fraction, NK cells activated fraction, NK cells resting fraction, plasma cells fraction, T cells CD4 memory activated fraction, T cells CD4 memory resting fraction, T cells CD8 fraction, T cells follicular helper fraction, T cells gamma delta fraction, and T cells regulatory (Tregs) fraction.

## Results

### Analysis of DE-miRNAs

Totally, 55 downregulated and 181 upregulated miRNAs were screened out in EC samples (**Supplemental Fig. 1a**). **Supplemental Fig. 1b** shows the heat map of DE-miRNAs.

### Target genes prediction of DE-miRNAs

DE-miRNA-gene pairs presenting in three databases were chosen to obtain reliable miRNA–gene pairs. As a result, 1927 target genes were selected for upregulated miRNAs and 1029 target genes for downregulated miRNAs (**Supplemental Table 2**).

### Identification of candidate DE-mRNAs and corresponding target genes

Totally, 3804 downregulated and 7727 upregulated mRNAs were screened out, and the corresponding target genes were also confirmed (**Supplemental Fig. 2a**). The heat map of DE-mRNAs was presented in **Supplemental Fig. 2b**.

**Differentially expressed genes**

Abundant studies have proved the inverse relationship between miRNAs and target genes[23]. Our study screened out 1927 target genes for upregulated miRNAs and 1029 target genes for downregulated miRNAs. 7727 upregulated and 3804 downregulated target genes of DE-mRNAs were identified. After analyzing DE-mRNAs and target genes of DE-miRNAs, 275 and 118 candidate DEGs for upregulated and downregulated DE-miRNAs were identified, respectively **(Fig. 2)**.

**Functional and pathway enrichment analysis**

GO and KEGG pathway enrichment analyses were applied for the functions of target genes. The GO functional annotation included BP, CC, and MF. **Fig. 3** presents the top 10 enriched GO items. In BP analysis, the candidate target genes of the upregulated DE-miRNAs were significantly enriched in the regulation of cell migration involved in sprouting angiogenesis and the negative regulation of DNA-templated transcription (**Fig. 3a**). In CC analysis, these genes were significantly enriched in chromatin and protein kinase complex (**Fig. 3c**). The MF analysis of these genes included vascular endothelial growth factor-activated receptor activity and transcriptional factor activity of RNA polymerase II core promoter proximal region sequence-specific binding (**Fig. 3e**). BP analysis showed that the candidate target genes of downregulated DE-miRNAs were positive and negative feedback regulation of DNA-templated transcription (**Fig. 3b**). In CC analysis, these genes were

significantly enriched in nuclear transcription factor complex and chromatin in telomeric region (**Fig. 3d**). MF analysis indicated that these genes were significantly enriched in AT DNA binding and retinoid X receptor binding (**Fig. 3f**). KEGG pathway enrichment analysis was performed for candidate target genes of upregulated and downregulated DE-miRNAs. The significant enrichment of candidate target genes of upregulated DE-miRNAs was found in FOXO signaling pathway, and Focal adhesion (**Fig. 3g**). For potential target genes of downregulated DE-miRNAs, the pathways in microRNAs in cancer, and cell cycle were enriched (**Fig. 3h**).

**Construction of PPI network and screening of hub genes**

After mapping these candidate DEGs into the STRING database, we constructed PPI network of these genes (**Fig. 4**). 275 and 118 node pairs of upregulated and downregulated DE-miRNAs for candidate target genes were obtained, respectively. The top 10 hub genes of upregulated DE-miRNAs were listed in **Supplemental Fig. 3a**. The top 10 hub genes of downregulated DE-miRNAs were showed in **Supplemental Fig. 4b**.

**Hub gene expression levels**

Using GEPIA database, we found the expression of the 10 hub genes of downregulated DE-miRNAs was significantly higher in EC tissues than those in normal ones **(Fig. 5)**. Marked upregulation was found in 7 out of 10 hub genes of upregulated DE-miRNAs in EC tissues compared with normal tissues. No significant

difference was observed in MYC, PRKACB, and GATA4 expression between the EC and normal tissues ($p > 0.05$).

**Identification of miRNA-mRNA regulatory pathways and corresponding transcription factors**

We established a miRNA-mRNA regulatory network of EC occurrence and progression (**Fig. 6**). Different genes might be regulated by the same miRNA. For example, miR-424-5p targeted the largest number of genes (KIF23, CHEK1, CEP55, CDC25A, and CCNE1) in the present regulatory network, suggesting that miR-424-5p may play a significant part in the development of EC. Furthermore, different miRNAs could regulate the same gene, indicating a vital role in the progression of EC. For example, NR3C1, FOXO1, and JUN were respectively targeted by the three miRNAs. Via FunRich software, the top five transcription factors for upregulated and downregulated DE-miRNAs were obtained (**Fig. 6b-c**).

Since 12 of the 18 miRNAs in the network have been verified in EC and their expression levels are consistent with our results, we assessed the remaining six miRNAs in EC. The results demonstrated that expression levels of miRNA-18a-5p, miRNA-18b-5p, miRNA-449c-5p and miRNA-1224-5p were markedly upregulated in EC tumors compared with that in paratumor tissues (**Fig. 7**). Of note, miRNA-636 expression was significantly downregulated, which was inconsistent with our prediction. The expression of miRNA-6715a-3p in EC was also detected (**Fig. 7f**), showing no significant differences between EC tissues and adjacent normal tissues.

Next, we investigated the expression levels of the corresponding target genes in EC. Results of the qRT-PCR revealed that NR3C1, CTGF, MYC, TNS1, PRKACB, and FOXO1 had a higher expression in tumors than in paratumor tissues (**Fig. 7j-l**). The above results indicated that miRNA-18a-5p, miRNA-18b-5p, miRNA-449c-5p and miRNA-1224-5p and their target genes in EC might play a greater functional role than miRNA-636 and miRNA-6715a-3p and their target genes.

**Construction of prognostic signature model**

A prognostic analysis was conducted on the 20 hub genes (**Supplemental Fig. 3**). The top eight significant prognostic factors were ESPL1, NR3C1, CCNE1, GATA4, KIF23, EZH2, CDC25A, and BIRC5 as shown in the univariate Cox proportional hazards regression analysis (**Supplemental Table 3**). The genes NR3C1, EZH2, and GATA4 exhibited a significant prognostic value in the multivariate Cox proportional hazards regression analysis. The hazard ratios of these three genes were positive, suggesting their negative correlation with prognosis. The following formula was used to calculate the patient's risk score:

Risk score = 0.284183* NR3C1 + 0.401466* EZH2 + 0.089382* GATA4

The patients fell into a high-risk group and a low-risk group based on the median risk score. Kaplan–Meier curve was plotted to compare the survival time of the low-risk patients and that of the high-risk patients. The results showed that the low-risk patients had significantly longer overall survival time than the high-risk ones ($p$< 0.0001; **Fig. 8a**). The areas under the time-dependent survival ROC curves were both

more than 0.656, indicating the good performance of our risk model in predicting 1-, 3-, and 5-year survival in the TCGA data set (**Fig. 8b**). We also analyzed the risk score distribution, survival status, and the expression of three genes for each patient (**Fig. 8c-e**). The heatmap (**Fig. 9a**) showed comparison of clinicopathological features between the two groups. Significant differences were found between the high-risk group and the low-risk group in terms of grade, age, stage, histological type and tumor status ($p < 0.01$). Univariate Cox regression analysis and multivariate Cox regression analysis proved that this prognostic model could be an independent prognostic indicator of EC (**Fig. 9b-c**). It was also found that high-risk patients in age ≥60 years old and stage III/IV subgroups were prone to an unfavorable OS (**Fig. 9d-e**). A nomogram was then constructed to predict 1-year, 3-year, and 5-year OS in 482 EC patients using seven prognostic factors including age, race, stage, histological type, grade, tumor status, and the risk score (**Fig. 10**). The nomogram, combined with the model, might be used to predict survival time of EC patients in clinical practice.

**The prognostic signature associated with immune cells infiltration**

We used CIBERSORT method to search the most significant tumor-infiltrating immune cells and prognostic signature of risk score. Three genes were found to be important in the enumeration and activation status of immune cell subtypes. Our exploration into the relationship between the risk score and the significant immune cell based on the three genes confirmed the close relationship between the three genes and the eight types of immune infiltration cell, including B cells naive fraction,

Macrophages M1 fraction, Neutrophils fraction, T cells CD4 memory resting fraction, T cells follicular helper fraction, T cells gamma delta fraction, and T cells regulatory (Tregs) fraction (**Fig. 11a-g**).

## Discussion

In recent years, quite a few studies have mentioned that the change of miRNAs and their downstream target gene expression is closely related to EC. However, so far, an integrated miRNA-mRNA regulatory network of EC has not been established. In the present study, we constructed the regulatory network between EC-associated genes and DE-miRNAs. Besides, we built a prognostic model based on hub genes, and confirmed the relationship between immune cell infiltration and the prognostic signature of risk score.

In our study, differential expression analysis was performed using miRNA and mRNA data from TCGA database. Five downregulated DE-miRNAs and 13 upregulated DE-miRNAs were finally determined, among which miR-424-5p targeted the largest number of genes (KIF23, CHEK1, CEP55, CDC25A, and CCNE1) in the regulatory network, suggesting the significant role of miR-424-5p in the occurrence and development of EC. Our analytic results on the expression of DE-miRNAs were mostly consistent with the previous studies. For example, the miR-424-5p and let-7c-5p expression levels were lower in EC tissues than in normal tissue samples [24, 25]. The significant down-regulation of miR-542-3p in EC[26, 27] promoted the

morphological change of endometrial stromal cells[28]. Lower expression of miR-101-3p was significantly correlated with poor overall survival; miR-101-3p affected cell proliferation and could control the carcinogenesis in endometrial serous carcinoma[29]. miR-96-5p, miR-182, miR-7, and miR-183-5p were significantly up-regulated in EC compared with normal endometrium[30, 31]. The miR-200 family (miR-200b, miR-200c, and miR-429) in EC was upregulated compared with that in normal endometrial tissues[32]. Li et al. identified that miRNA-29c-3p (a tumor suppressor) was significantly lower in the EC cells and linked to the low paclitaxel sensitivity of EC [33]. However, some miRNAs were found to be linked to other tumors rather than EC. For instance, a research revealed the significantly higher expression of miR-636 and the significantly lower expression of miR-18a-5p in breast cancer than in normal samples[34]. Wu et al. detected lower miR-449c-5p levels in gastric cancer (GC), which was correlated with a lower survival rate[35]. miR-18b-5p was upregulated in breast cancer[36, 37]. Compared with normal tissues, miR-1224-5p was significantly down-regulated in lung cancer tissues[38]. Although most miRNAs in the network have been reported to be associated with cancer, miR-6715a-3p has not yet been reported. According to the present network, miR-6715a-3p might be related to EC. However, further qRT-PCR found higher expression of miR-6715a-3p in EC tissues than in the adjacent tissues with no significant difference, which might be caused by the small sample size.

We built the PPI network and identified the top 20 hub genes (10 upregulated and 10

downregulated ones). The expressions of these hub genes in EC were assessed using GEPIA database, which included more normal samples than TCGA [19]. Inspiringly, the expression levels of these genes were generally consistent with our results of TCGA mRNA data. Most of these genes were key modulators of EC. For example, c-myc was found activated in multiple human tumors (including EC) with a poor disease prognosis [39, 40]; c-myc has been proved to promote EC growth through many pathways[41-43]. The histone methyltransferase EZH2 promoted EC cell growth through H3K27 trimethylation[44]. CCNA2 knockdown decreased the cell proliferation in human EC cell lines[45]. Based on the above results, we built a miRNA-mRNA regulatory network. In this network, most miRNA-mRNA pairs, which might contribute to the pathogenesis of EC, are potential therapeutic targets and deserve further exploration.

Since miRNA expression is modulated by transcription factors[46, 47], we speculated that these DE-miRNAs could be regulated by the transcription factors. Specific protein-1 (Sp1), a zinc-finger transcription factor of the Sp/KLF family, can bind to GC-rich promoter elements like GC-boxes, CACCC-boxes and related motif [48-50]. Sp1 regulates the expression of genes involved in cell cycle, proliferation and death[51, 52] and has been widely reported as a miRNA target[53, 54]. But few studies have reported its role in miRNA expression modulation and its function in EC. For instance, Sp1 was verified as a target of miR-490, and Sp1 knockdown could reverse the effects of miR-490 inhibition on the malignant behaviors of EC, providing

a new strategy for EC therapy[55]. The functions of these transcription factors in EC need more experimental exploration in the future.

In this study, we developed a three-gene signature (GATA4, NR3C1, and EZH2) from the 20 hub genes. These three key genes are correlated to tumorigenesis, development and metastasis. The abnormal expression of GATA4 are reported to be associated with onset and progression of some solid tumors, but whether GATA4 is an oncogenic driver or a tumor suppressor in oncogenesis is unclear. Chia et al.[56] found that KLF5/GATA4/GATA6 might promote gastric cancer (GC) development by engaging in mutual crosstalk, maintaining a pro-oncogenic transcriptional regulatory network in GC. A recent study also demonstrated that GATA4 promoted oncogenesis by inhibiting miR125b-dependent suppression of DKK3 expression[57]. However, Han et al. discovered that GATA4 could suppress tumor by repressing the NF-κB signaling in cells of breast cancer[58]. Compared with samples of non-neoplastic endometrium, the EC group showed significant higher methylation in GATA4 gene[59]. In addition, nuclear receptor subfamily 3 group C member 1 (NR3C1), a member of the nuclear hormone receptor super family of ligand-activated transcription factors, regulates the glucocorticoid hormone effects and leads to changed gene expression in target cells and tissues[60]. NR3C1 was identified as epigenetically deregulated gene in gastrointestinal tumorigenesis[61, 62]. It was also found that NR3C1expression was correlated with liver metastasis of GC [63]. NR3C1 was highly methylated in GC, which might play a pivotal role in the initiation and progression of GC, and the

variants of NR3C1, namely rs4912913, rs33388 and rs12521436, might contribute to GC susceptibility[64, 65]. Besides, EZH2, the enzymatic subunit of the polycomb-repressive complex 2 (PRC2) that catalyzes H3K27 methylation, is a most frequently mutated epigenetic regulator in hematologic malignancies. A recent study, indicated that EZH2, as a potential anti-EC therapeutic target, could drive EC progression by regulating miR-361/Twist signaling, which is consistent with our research [66]. These findings suggest that the three-genes signature can help clinicians to select high-risk patients from those with identical clinical or molecular characteristics and make rational treatment decisions.

EC is a group of heterogeneous tumors with distinct characteristics. The development of high-throughput technologies enables the targeted therapies of EC. However, few targeted therapies have been applied in clinical practice. Currently, immunotherapy is changing the treatment of EC. Therefore, it is critical to identify molecular subgroups that are amenable to targeted therapies, including immunotherapy. We established a prognostic model to compare the enumeration and activation status of immune cell subtypes between high-risk and low-risk groups. Many studies have supported the key role of immune cells infiltration in the occurrence and progress of cancer. For example, T cells can induce dormancy or promote multistage carcinogenesis. The degree of T cell infiltration in tumor is an important predictor of the patient's response to cancer immunotherapy[67]. High T cell density in tumor and immune cells is often considered as an active anti-tumor response[68]. Tumor-associated macrophages

become tumoricidal if they are in a less hypoxic environment and less exposed to tumor-derived cytokines, which might occur in the presence of a significant number of M1 macrophages[69, 70]. Besides, in the advanced stage of tumor, M1 macrophages tend to polarize into M2 macrophages, thus having protumor function[71].

The present study has some limitations. First, the sample size in TCGA database is not large enough. Second, the association of these miRNA-mRNA pairs needs to be validated in experiments. In the future, more in vitro and in vivo functional experiments should be performed on the miRNA-mRNA regulatory pathways in EC.

## Conclusions

The miRNA-mRNA regulatory network in EC was established and three hub genes were screened out from hundreds of candidate genes by bioinformatics analysis. Moreover, we identified a three-gene prognostic signature as a prognostic predictor for EC. The findings of this study may provide theoretical reference for the exploration of the biomarkers for the diagnosis and prognosis of EC.

## Abbreviations

EC: endometrial cancer; DE-miRNAs: differentially expressed; DE-mRNAs: differentially expressed mRNAs; DEGs: the differentially expressed genes; FC: fold change; GO: gene ontology; KEGG: The Kyoto Encyclopedia of Genes and Genomes;

BP: biological process; CC: cellular component; MF: molecular function; microRNAs: microRNAs; mRNAs: messagerRNAs; PPI: protein–protein interaction; FDR: false discovery rate; AUC: area under curve; ROC: Receiver operating characteristic.

**Acknowledgements**

The authors would like to express our sincere thanks for sharing the data from The Cancer Genome Atlas (TCGA) database.

**Authors' contributions**

JL and WC conceived and designed this study. RS and SN wrote this manuscript. YJ and SL revised this manuscript. JY made these figures.

**Funding**

This work was supported by the National Natural Science Foundation of China (8187101839).

**Availability of data and materials**

Not applicable.

**Ethics approval and consent to participate**

The clinical program was approved by the ethics committee of the First Affiliated Hospital with Nanjing Medical University. All patients individually signed informed

consent.

## Consent for publication

All parties consented for publication.

## Competing interests

The authors declare that they have no competing interests.

## References


1. Chu D, Wu J, Wang K, Zhao M, Wang C, Li L, Guo R: Effect of metformin use on the risk and prognosis of endometrial cancer: a systematic review and meta-analysis. *Bmc Cancer* 2018, 18:438.

2. Morice P, Leary A, Creutzberg C, Abu-Rustum N, Darai E: Endometrial cancer. *Lancet* 2016, 387:1094-1108.

3. Lee YC, Lheureux S, Oza AM: Treatment strategies for endometrial cancer: current practice and perspective. *Curr Opin Obstet Gynecol* 2017, 29:47-58.

4. Ramon LA, Braza-Boils A, Gilabert J, Chirivella M, Espana F, Estelles A, Gilabert-Estelles J: microRNAs related to angiogenesis are dysregulated in endometrioid endometrial cancer. *Hum Reprod* 2012, 27:3036-3045.

5. Yan R, Yang T, Zhai H, Zhou Z, Gao L, Li Y: MicroRNA-150-5p affects cell proliferation, apoptosis, and EMT by regulation of the BRAF(V600E) mutation in papillary thyroid cancer cells. *J Cell Biochem* 2018, 119:8763-8772.

6. Yang Z, Zhang T, Wang Q, Gao H: Overexpression of microRNA-34a Attenuates Proliferation

and Induces Apoptosis in Pituitary Adenoma Cells via SOX7. *Mol Ther Oncolytics* 2018, 10:40-47.

7. Li P, Xie XB, Chen Q, Pang GL, Luo W, Tu JC, Zheng F, Liu SM, Han L, Zhang JK, et al: MiRNA-15a mediates cell cycle arrest and potentiates apoptosis in breast cancer cells by targeting synuclein-gamma. *Asian Pac J Cancer Prev* 2014, 15:6949-6954.

8. Xiao R, Li C, Chai B: miRNA-144 suppresses proliferation and migration of colorectal cancer cells through GSPT1. *Biomed Pharmacother* 2015, 74:138-144.

9. Dotto GP, Karine L: miR-34a/SIRT6 in squamous differentiation and cancer. *Cell Cycle* 2014, 13:1055-1056.

10. Si W, Shen J, Du C, Chen D, Gu X, Li C, Yao M, Pan J, Cheng J, Jiang D, et al: A miR-20a/MAPK1/c-Myc regulatory feedback loop regulates breast carcinogenesis and chemoresistance. *Cell Death Differ* 2018, 25:406-420.

11. Carreras-Badosa G, Bonmati A, Ortega FJ, Mercader JM, Guindo-Martinez M, Torrents D, Prats-Puig A, Martinez-Calcerrada JM, Platero-Gutierrez E, De Zegher F, et al: Altered Circulating miRNA Expression Profile in Pregestational and Gestational Obesity. *J Clin Endocrinol Metab* 2015, 100:E1446-E1456.

12. Ohlsson TE, Van der Hoek KH, Van der Hoek MB, Perry N, Wagaarachchi P, Robertson SA, Print CG, Hull LM: MicroRNA-regulated pathways associated with endometriosis. *Mol Endocrinol* 2009, 23:265-275.

13. Sonkoly E, Pivarcsi A: microRNAs in inflammation. *Int Rev Immunol* 2009, 28:535-561.

14. Joladarashi D, Thandavarayan RA, Babu SS, Krishnamurthy P: Small engine, big power: microRNAs as regulators of cardiac diseases and regeneration. *Int J Mol Sci* 2014, 15:15891-15911.

15. Ramon LA, Braza-Boils A, Gilabert-Estelles J, Gilabert J, Espana F, Chirivella M, Estelles A:

microRNAs expression in endometriosis and their relation to angiogenic factors. *Hum Reprod* 2011, 26:1082-1090.

16. Gilabert-Estelles J, Braza-Boils A, Ramon LA, Zorio E, Medina P, Espana F, Estelles A: Role of microRNAs in gynecological pathology. *Curr Med Chem* 2012, 19:2406-2413.

17. Cohn DE, Fabbri M, Valeri N, Alder H, Ivanov I, Liu CG, Croce CM, Resnick KE: Comprehensive miRNA profiling of surgically staged endometrial cancer. *Am J Obstet Gynecol* 2010, 202:651-656.

18. Zhang W, Chen JH, Shan T, Aguilera-Barrantes I, Wang LS, Huang TH, Rader JS, Sheng X, Huang YW: miR-137 is a tumor suppressor in endometrial cancer and is repressed by DNA hypermethylation. *Lab Invest* 2018, 98:1397-1407.

19. Tang Z, Li C, Kang B, Gao G, Li C, Zhang Z: GEPIA: a web server for cancer and normal gene expression profiling and interactive analyses. *Nucleic Acids Res* 2017, 45:W98-W102.

20. Zhang Z: Semi-parametric regression model for survival data: graphical visualization with R. *Ann Transl Med* 2016, 4:461.

21. Iasonos A, Schrag D, Raj GV, Panageas KS: How to build and interpret a nomogram for cancer prognosis. *J Clin Oncol* 2008, 26:1364-1370.

22. Newman AM, Liu CL, Green MR, Gentles AJ, Feng W, Xu Y, Hoang CD, Diehn M, Alizadeh AA: Robust enumeration of cell subsets from tissue expression profiles. *Nat Methods* 2015, 12:453-457.

23. Hammond SM: An overview of microRNAs. *Adv Drug Deliv Rev* 2015, 87:3-14.

24. Lu Z, Nian Z, Jingjing Z, Tao L, Quan L: MicroRNA-424/E2F6 feedback loop modulates cell invasion, migration and EMT in endometrial carcinoma. *Oncotarget* 2017, 8:114281-114291.

25. Xiong H, Li Q, Liu S, Wang F, Xiong Z, Chen J, Chen H, Yang Y, Tan X, Luo Q, et al: Integrated microRNA and mRNA transcriptome sequencing reveals the potential roles of miRNAs in stage I endometrioid endometrial carcinoma. *Plos One* 2014, 9:e110163.

26. Jurcevic S, Olsson B, Klinga-Levan K: MicroRNA expression in human endometrial adenocarcinoma. *Cancer Cell Int* 2014, 14:88.

27. Devor EJ, Cha E, Warrier A, Miller MD, Gonzalez-Bosquet J, Leslie KK: The miR-503 cluster is coordinately under-expressed in endometrial endometrioid adenocarcinoma and targets many oncogenes, cell cycle genes, DNA repair genes and chemotherapy response genes. *Onco Targets Ther* 2018, 11:7205-7211.

28. Tochigi H, Kajihara T, Mizuno Y, Mizuno Y, Tamaru S, Kamei Y, Okazaki Y, Brosens JJ, Ishihara O: Loss of miR-542-3p enhances IGFBP-1 expression in decidualizing human endometrial stromal cells. *Sci Rep* 2017, 7:40001.

29. Hiroki E, Akahira J, Suzuki F, Nagase S, Ito K, Suzuki T, Sasano H, Yaegashi N: Changes in microRNA expression levels correlate with clinicopathological features and prognoses in endometrial serous adenocarcinomas. *Cancer Sci* 2010, 101:241-249.

30. Myatt SS, Wang J, Monteiro LJ, Christian M, Ho KK, Fusi L, Dina RE, Brosens JJ, Ghaem-Maghami S, Lam EW: Definition of microRNAs that repress expression of the tumor suppressor gene FOXO1 in endometrial cancer. *Cancer Res* 2010, 70:367-377.

31. Chung TK, Lau TS, Cheung TH, Yim SF, Lo KW, Siu NS, Chan LK, Yu MY, Kwong J, Doran G, et al: Dysregulation of microRNA-204 mediates migration and invasion of endometrial cancer by regulating FOXC1. *Int J Cancer* 2012, 130:1036-1045.

32. Lee JW, Park YA, Choi JJ, Lee YY, Kim CJ, Choi C, Kim TJ, Lee NW, Kim BG, Bae DS: The

expression of the miRNA-200 family in endometrial endometrioid carcinoma. *Gynecol Oncol* 2011, 120:56-62.

33. Li L, Shou H, Wang Q, Liu S: Investigation of the potential theranostic role of KDM5B/miR-29c signaling axis in paclitaxel resistant endometrial carcinoma. *Gene* 2019, 694:76-82.

34. Encarnacion-Medina J, Ortiz C, Vergne R, Padilla L, Matta J: MicroRNA Expression Changes in Women with Breast Cancer Stratified by DNA Repair Capacity Levels. *J Oncol* 2019, 2019:7820275.

35. Wu Z, Wang H, Fang S, Xu C: MiR-449c inhibits gastric carcinoma growth. *Life Sci* 2015, 137:14-19.

36. Fonseca-Sanchez MA, Perez-Plasencia C, Fernandez-Retana J, Arechaga-Ocampo E, Marchat LA, Rodriguez-Cuevas S, Bautista-Pina V, Arellano-Anaya ZE, Flores-Perez A, Diaz-Chavez J, Lopez-Camarillo C: microRNA-18b is upregulated in breast cancer and modulates genes involved in cell migration. *Oncol Rep* 2013, 30:2399-2410.

37. Hong Y, Liang H, Uzair-Ur-Rehman, Wang Y, Zhang W, Zhou Y, Chen S, Yu M, Cui S, Liu M, et al: miR-96 promotes cell proliferation, migration and invasion by targeting PTPN9 in breast cancer. *Sci Rep* 2016, 6:37421.

38. Yu PF, Wang Y, Lv W, Kou D, Hu HL, Guo SS, Zhao YJ: LncRNA NEAT1/miR-1224/KLF3 contributes to cell proliferation, apoptosis and invasion in lung cancer. *Eur Rev Med Pharmacol Sci* 2019, 23:8403-8410.

39. Dang CV: c-Myc target genes involved in cell growth, apoptosis, and metabolism. *Mol Cell Biol* 1999, 19:1-11.

40. Geisler JP, Geisler HE, Manahan KJ, Miller GA, Wiemann MC, Zhou Z, Crabtree W: Nuclear and cytoplasmic c-myc staining in endometrial carcinoma and their relationship to survival. *Int J*

*Gynecol Cancer* 2004, 14:133-137.

41. Subramaniam KS, Omar IS, Kwong SC, Mohamed Z, Woo YL, Mat AN, Chung I: Cancer-associated fibroblasts promote endometrial cancer growth via activation of interleukin-6/STAT-3/c-Myc pathway. *Am J Cancer Res* 2016, 6:200-213.

42. Qiu MT, Fan Q, Zhu Z, Kwan SY, Chen L, Chen JH, Ying ZL, Zhou Y, Gu W, Wang LH, et al: KDM4B and KDM4A promote endometrial cancer progression by regulating androgen receptor, c-myc, and p27kip1. *Oncotarget* 2015, 6:31702-31720.

43. Bai JX, Yan B, Zhao ZN, Xiao X, Qin WW, Zhang R, Jia LT, Meng YL, Jin BQ, Fan DM, et al: Tamoxifen represses miR-200 microRNAs and promotes epithelial-to-mesenchymal transition by up-regulating c-Myc in endometrial carcinoma cell lines. *Endocrinology* 2013, 154:635-645.

44. Oki S, Sone K, Oda K, Hamamoto R, Ikemura M, Maeda D, Takeuchi M, Tanikawa M, Mori-Uchino M, Nagasaka K, et al: Oncogenic histone methyltransferase EZH2: A novel prognostic marker with therapeutic potential in endometrial cancer. *Oncotarget* 2017, 8:40402-40411.

45. Huo X, Sun H, Cao D, Yang J, Peng P, Yu M, Shen K: Identification of prognosis markers for endometrial cancer by integrated analysis of DNA methylation and RNA-Seq data. *Sci Rep* 2019, 9:9924.

46. Mullany LE, Herrick JS, Wolff RK, Stevens JR, Samowitz W, Slattery ML: MicroRNA-transcription factor interactions and their combined effect on target gene expression in colon cancer cases. *Genes Chromosomes Cancer* 2018, 57:192-202.

47. Mullany LE, Herrick JS, Wolff RK, Stevens JR, Samowitz W, Slattery ML: Transcription factor-microRNA associations and their impact on colorectal cancer survival. *Mol Carcinog* 2017, 56:2512-2526.

48. Lania L, Majello B, De Luca P: Transcriptional regulation by the Sp family proteins. *Int J Biochem Cell Biol* 1997, 29:1313-1323.

49. Yu JH, Schwartzbauer G, Kazlman A, Menon RK: Role of the Sp family of transcription factors in the ontogeny of growth hormone receptor gene expression. *J Biol Chem* 1999, 274:34327-34336.

50. Suske G: The Sp-family of transcription factors. *Gene* 1999, 238:291-300.

51. Maor S, Mayer D, Yarden RI, Lee AV, Sarfstein R, Werner H, Papa MZ: Estrogen receptor regulates insulin-like growth factor-I receptor gene expression in breast tumor cells: involvement of transcription factor Sp1. *J Endocrinol* 2006, 191:605-612.

52. Tong Y, Tan Y, Zhou C, Melmed S: Pituitary tumor transforming gene interacts with Sp1 to modulate G1/S cell phase transition. *Oncogene* 2007, 26:5596-5605.

53. Hu J, Shan Z, Hu K, Ren F, Zhang W, Han M, Li Y, Feng K, Lei L, Feng Y: miRNA-223 inhibits epithelial-mesenchymal transition in gastric carcinoma cells via Sp1. *Int J Oncol* 2016, 49:325-335.

54. Qin F, Zhao Y, Shang W, Zhao ZM, Qian X, Zhang BB, Cai H: Sinomenine relieves oxygen and glucose deprivation-induced microglial activation via inhibition of the SP1/miRNA-183-5p/IkappaB-alpha signaling pathway. *Cell Mol Biol (Noisy-le-grand)* 2018, 64:140-147.

55. Shao W, Li Y, Chen F, Jia H, Jia J, Fu Y: Long non-coding RNA DLEU1 contributes to the development of endometrial cancer by sponging miR-490 to regulate SP1 expression. *Pharmazie* 2018, 73:379-385.

56. Chia NY, Deng N, Das K, Huang D, Hu L, Zhu Y, Lim KH, Lee MH, Wu J, Sam XX, et al: Regulatory crosstalk between lineage-survival oncogenes KLF5, GATA4 and GATA6 cooperatively promotes gastric cancer development. *Gut* 2015, 64:707-719.

57. Pei Y, Yao Q, Yuan S, Xie B, Liu Y, Ye C, Zhuo H: GATA4 promotes hepatoblastoma cell proliferation by altering expression of miR125b and DKK3. *Oncotarget* 2016, 7:77890-77901.

58. Han X, Tang J, Chen T, Ren G: Restoration of GATA4 expression impedes breast cancer progression by transcriptional repression of ReLA and inhibition of NF-kappaB signaling. *J Cell Biochem* 2019, 120:917-927.

59. Chmelarova M, Kos S, Dvorakova E, Spacek J, Laco J, Ruszova E, Hrochova K, Palicka V: Importance of promoter methylation of GATA4 and TP53 genes in endometrioid carcinoma of endometrium. *Clin Chem Lab Med* 2014, 52:1229-1234.

60. Sanchez-Vega B, Gandhi V: Glucocorticoid resistance in a multiple myeloma cell line is regulated by a transcription elongation block in the glucocorticoid receptor gene (NR3C1). *Br J Haematol* 2009, 144:856-864.

61. Ahlquist T, Lind GE, Costa VL, Meling GI, Vatn M, Hoff GS, Rognum TO, Skotheim RI, Thiis-Evensen E, Lothe RA: Gene methylation profiles of normal mucosa, and benign and malignant colorectal tumors identify early onset markers. *Mol Cancer* 2008, 7:94.

62. Lind GE, Kleivi K, Meling GI, Teixeira MR, Thiis-Evensen E, Rognum TO, Lothe RA: ADAMTS1, CRABP1, and NR3C1 identified as epigenetically deregulated genes in colorectal tumorigenesis. *Cell Oncol* 2006, 28:259-272.

63. Chang W, Ma L, Lin L, Gu L, Liu X, Cai H, Yu Y, Tan X, Zhai Y, Xu X, et al: Identification of novel hub genes associated with liver metastasis of gastric cancer. *Int J Cancer* 2009, 125:2844-2853.

64. Gu Y, Deng B, Kong J, Yan C, Huang T, Yang J, Wang Y, Wang T, Qi Q, Jin G, et al: Functional polymorphisms in NR3C1 are associated with gastric cancer risk in Chinese population. *Oncotarget* 2017, 8:105312-105319.

65. Qu Y, Dang S, Hou P: Gene methylation in gastric cancer. *Clin Chim Acta* 2013, 424:53-65.

66. Ihira K, Dong P, Xiong Y, Watari H, Konno Y, Hanley SJ, Noguchi M, Hirata N, Suizu F, Yamada T, et al: EZH2 inhibition suppresses endometrial cancer progression via miR-361/Twist axis. *Oncotarget* 2017, 8:13509-13520.

67. Teng MW, Ngiow SF, Ribas A, Smyth MJ: Classifying Cancers Based on T-cell Infiltration and PD-L1. *Cancer Res* 2015, 75:2139-2145.

68. Chen DS, Mellman I: Elements of cancer immunity and the cancer-immune set point. *Nature* 2017, 541:321-330.

69. Greten FR, Eckmann L, Greten TF, Park JM, Li ZW, Egan LJ, Kagnoff MF, Karin M: IKKbeta links inflammation and tumorigenesis in a mouse model of colitis-associated cancer. *Cell* 2004, 118:285-296.

70. Mantovani A, Sica A, Allavena P, Garlanda C, Locati M: Tumor-associated macrophages and the related myeloid-derived suppressor cells as a paradigm of the diversity of macrophage activation. *Hum Immunol* 2009, 70:325-330.

71. Dunn GP, Old LJ, Schreiber RD: The three Es of cancer immunoediting. *Annu Rev Immunol* 2004, 22:329-360.

## Fig. legends

**Fig. 1** Flow chart of this article.

**Fig. 2** Screening of candidate DEGs. (a) The intersection of target genes of upregulated DE-miRNAs and downregulated target genes of DE-mRNAs; (b) The

intersection of target genes of downregulated DE-miRNAs and upregulated target genes of DE-mRNAs. Blue represents target target genes of DE-miRNAs. Yellow represents DE-mRNAs.

**Fig. 3** The enriched functions for DEGs of DE-mRNAs and DE-miRNAs. (a) The top 10 enriched BP items of downregulated candidate genes; (b) the top 10 enriched BP items of upregulated candidate genes; (c) the top 10 enriched CC items of downregulated candidate genes; (d) the top 10 enriched CC items of upregulated candidate genes; (e) the top 10 enriched MF items of downregulated candidate genes; (f) the top 10 enriched MF items of upregulated candidate genes.

**Fig. 4** PPI network of the candidate target genes; (a) For upregulated DE-miRNAs; (b) For downregulated DE-miRNAs.

**Fig. 5** The expression levels of 17 hub genes from the GEPIA database. * $p < 0.05$.

**Fig. 6** Regulatory network of miRNA-mRNAs and corresponding transcription factors. (a)Regulatory network of RC-associated genes and their target miRNAs. miRNAs: microRNA; Red represents upregulation. Blue represents downregulation. The oval represents mRNA. The rectangle represents miRNA. (b) Predicted transcription factors of upregulated DE-miRNAs; (c) transcription factors of downregulated DE-miRNAs.

**Fig. 7** Expression of potential miRNAs and target genes in EC tissues and normal adjacent tissues. (a-f) miRNA expression levels (g-l) mRNA expression levels. *$p$<0.05. **$p$<0.01.

**Fig. 8** Analysis of the prognostic model between low- and high-risk groups. (a) Kapla-Meier survival curve of overall survival between the high-risk group and low-risk group; (b) The time-dependent survival ROC curves; (c) The distributions of risk score; (d) Survival status; (e) The heatmap shows the expression levels of the three genes in low- and high-risk groups.

**Fig. 9** Study of the factors impacting prognosis of EC. (a) The heatmap shows the distribution of clinicopathological features was compared between the low- and high-risk groups. ** $p$<0.01; *** $p$<0.001. (b) Forest Plot for univariate Cox regression analysis of clinical factors and risk score. (c) Forest Plot for multivariate Cox regression analysis of clinical factors and risk score. (d) Kaplan-Meier survival curve of age ≥60 years old subgroup between the low- and high-risk groups for the overall survival rate in endometrial carcinoma. (e) Kaplan-Meier survival curve of stage III/IV subgroup between the low- and high-risk groups for the overall survival rate in endometrial carcinoma.

**Fig. 10** Nomogram predicting overall survival for EC patients. (a) For each patient,

seven lines are drawn upward to determine the points received from the seven predictors in the nomogram. The sum of these points is located on the 'Points' axis. Then a line is drawn downward to determine the possibility of 1-, 3-, and 5-year overall survival of EC. (b) The calibration plot for internal validation of the nomogram. The Y-axis represents actual survival, and the X-axis represents nomogram-predicted survival.

**Fig. 11** The relationship of risk score with the significant immune cell. (a) B cells naive fraction. (b) Macrophages M1. (c) Neutrophils. (d) T cells regulatory (Tregs). (e) T cells CD4 memory resting. (f) T cells follicular helper. (g) T cells gamma delta.

# Figures

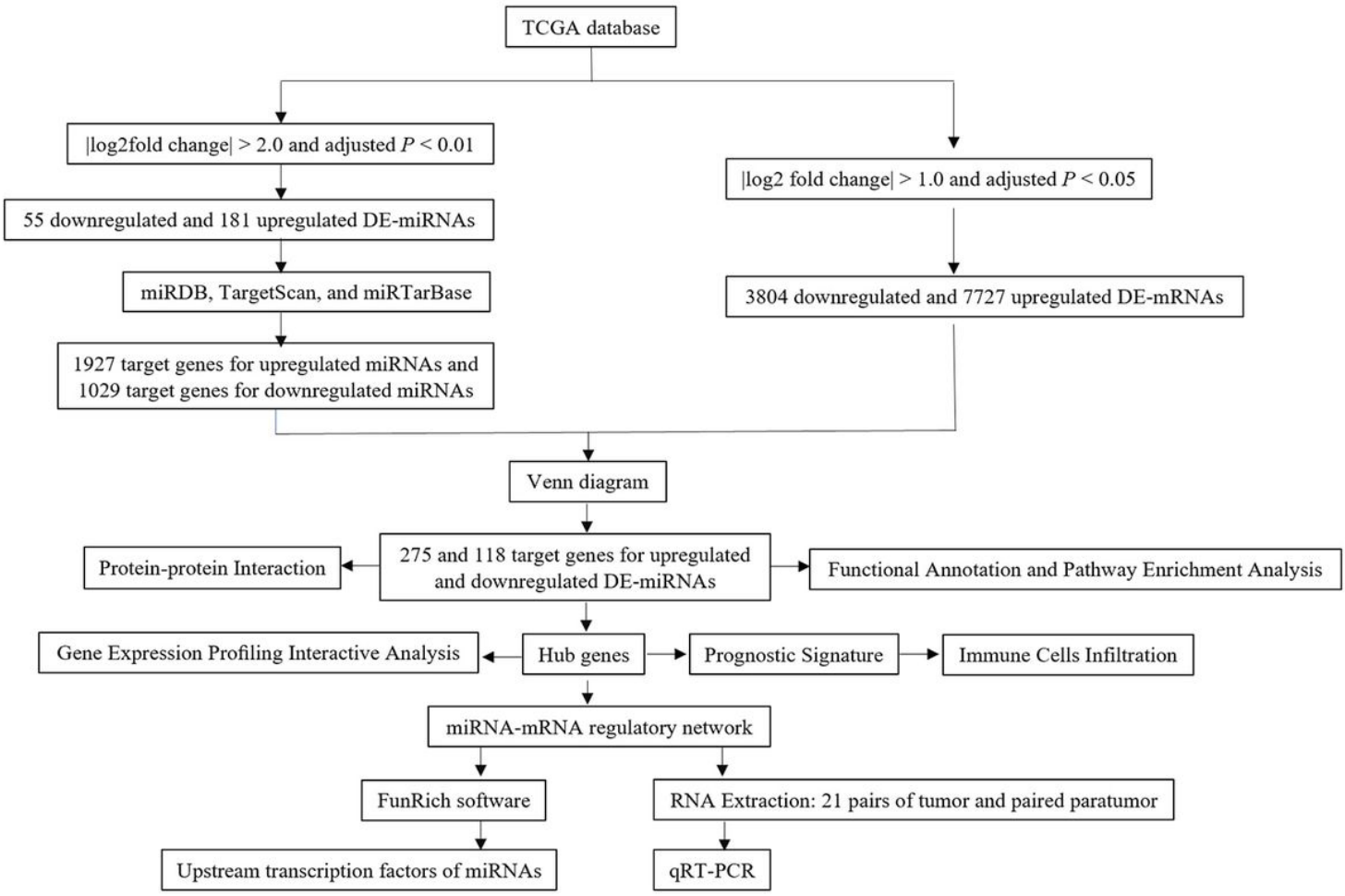


## Figure 2

Flow chart of this article.

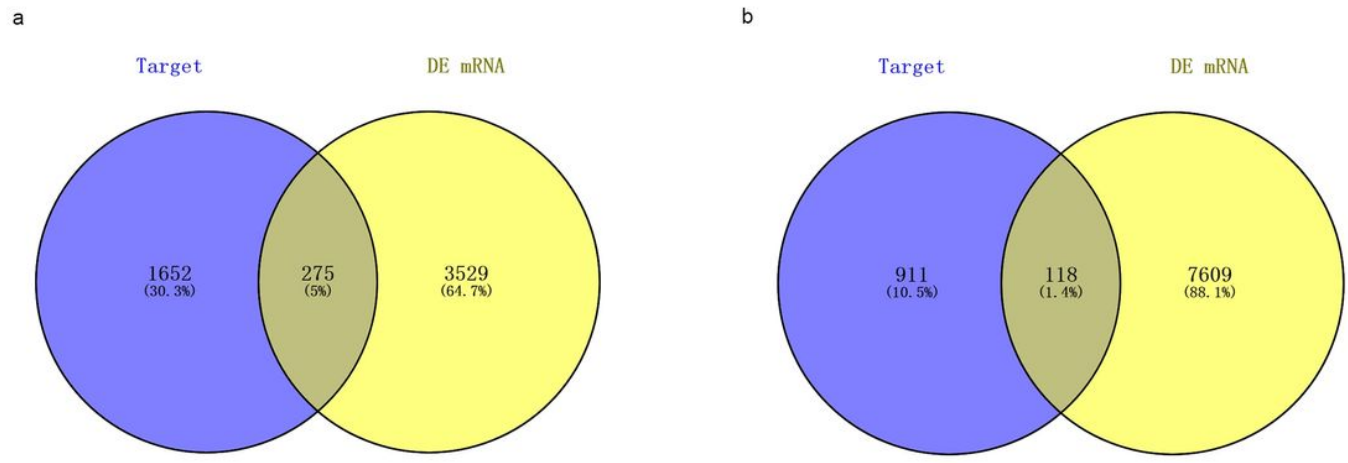

## Figure 4

Screening of candidate DEGs. (a) The intersection of target genes of upregulated DE-miRNAs and downregulated target genes of DE-mRNAs; (b) The 31 intersection of target genes of downregulated DE-miRNAs and upregulated target genes of DE-mRNAs. Blue represents target target genes of DE-miRNAs. Yellow represents DE-mRNAs.

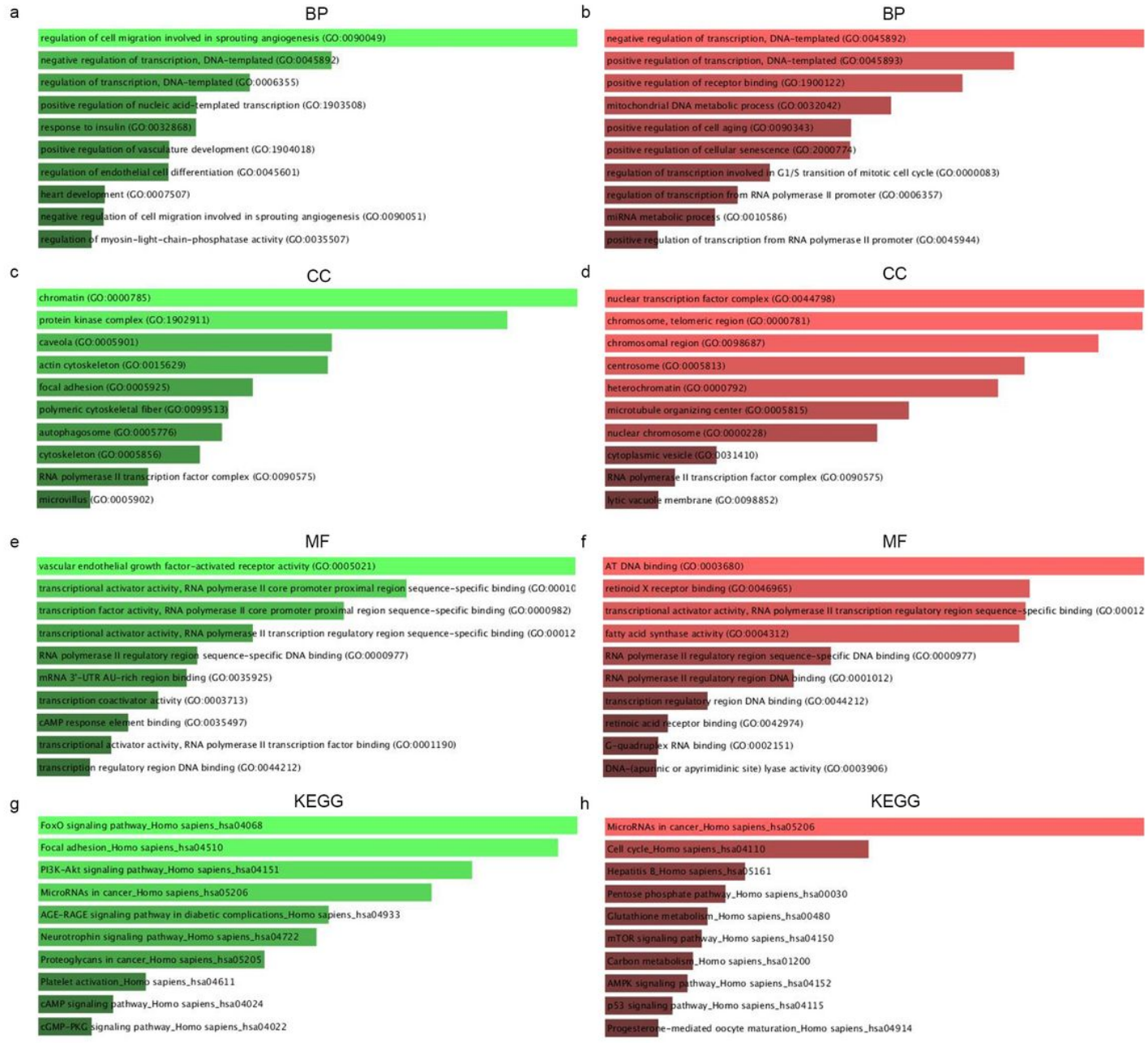


## Figure 6

The enriched functions for DEGs of DE-mRNAs and DE-miRNAs. (a) The top 10 enriched BP items of downregulated candidate genes; (b) the top 10 enriched BP items of upregulated candidate genes; (c) the top 10 enriched CC items of downregulated candidate genes; (d) the top 10 enriched CC items of

upregulated candidate genes; (e) the top 10 enriched MF items of downregulated candidate genes; (f) the top 10 enriched MF items of upregulated candidate genes.

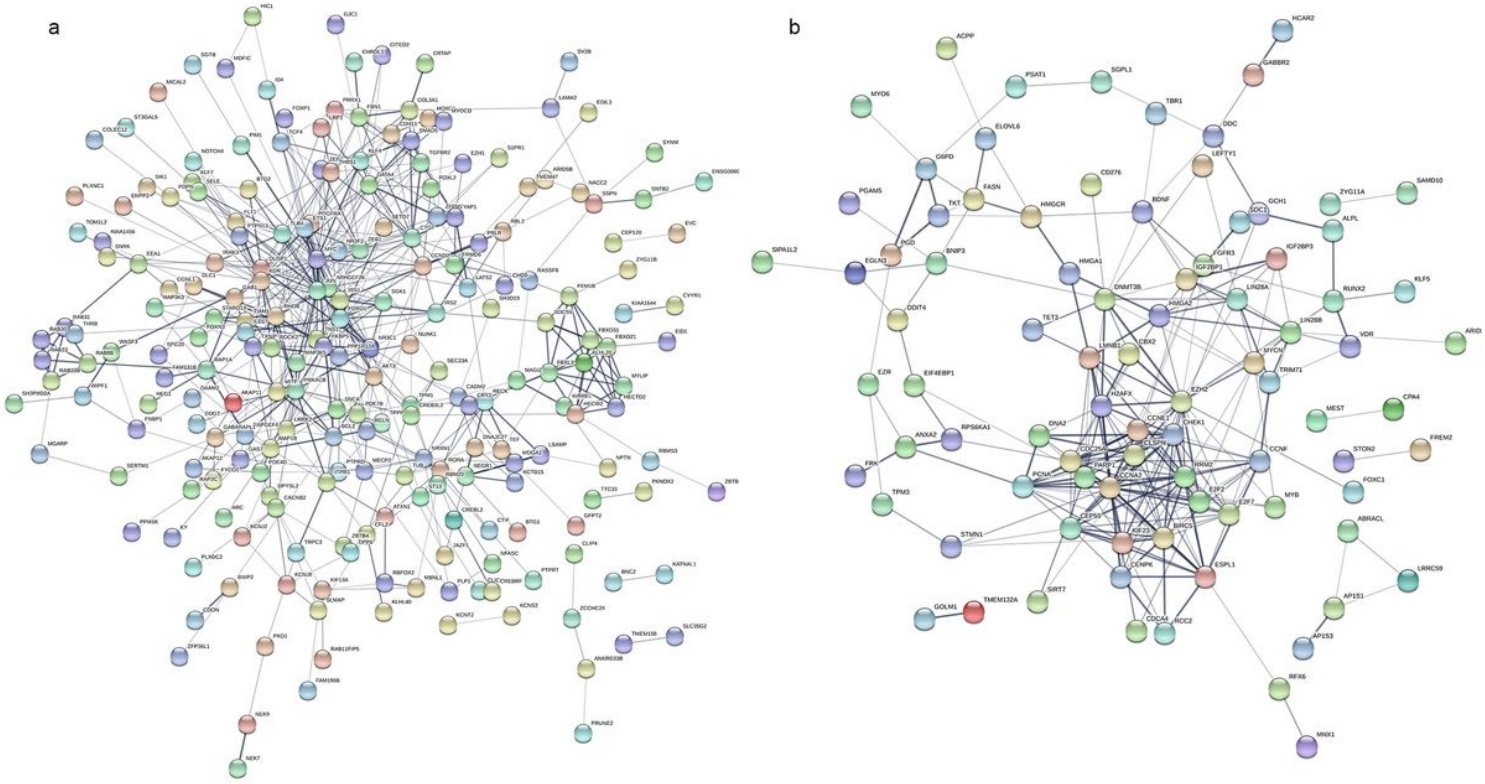


**Figure 8**

PPI network of the candidate target genes; (a) For upregulated DE-miRNAs; (b) For downregulated DE-miRNAs.

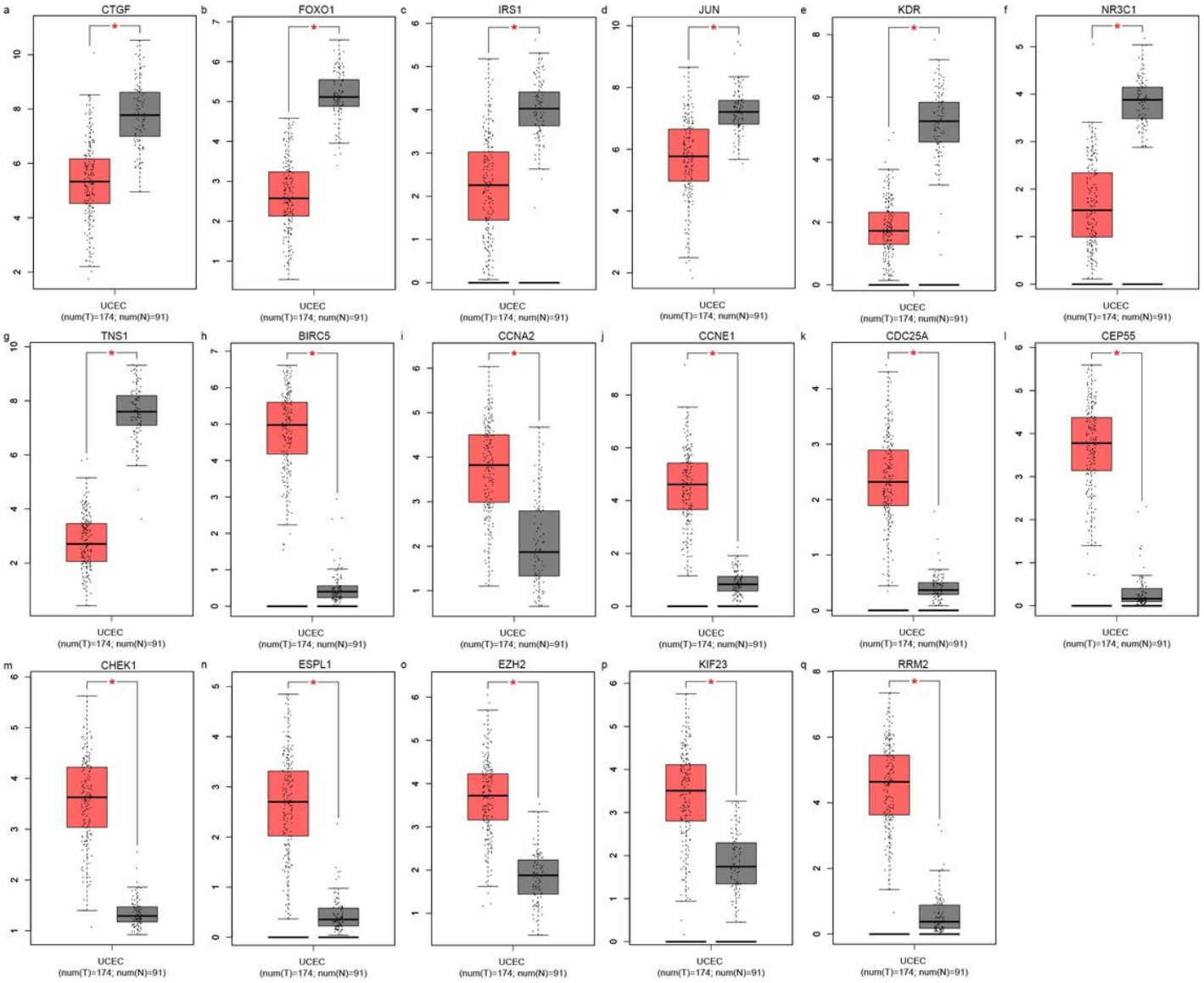


## Figure 10

The expression levels of 17 hub genes from the GEPIA database. * $p < 0.05$.

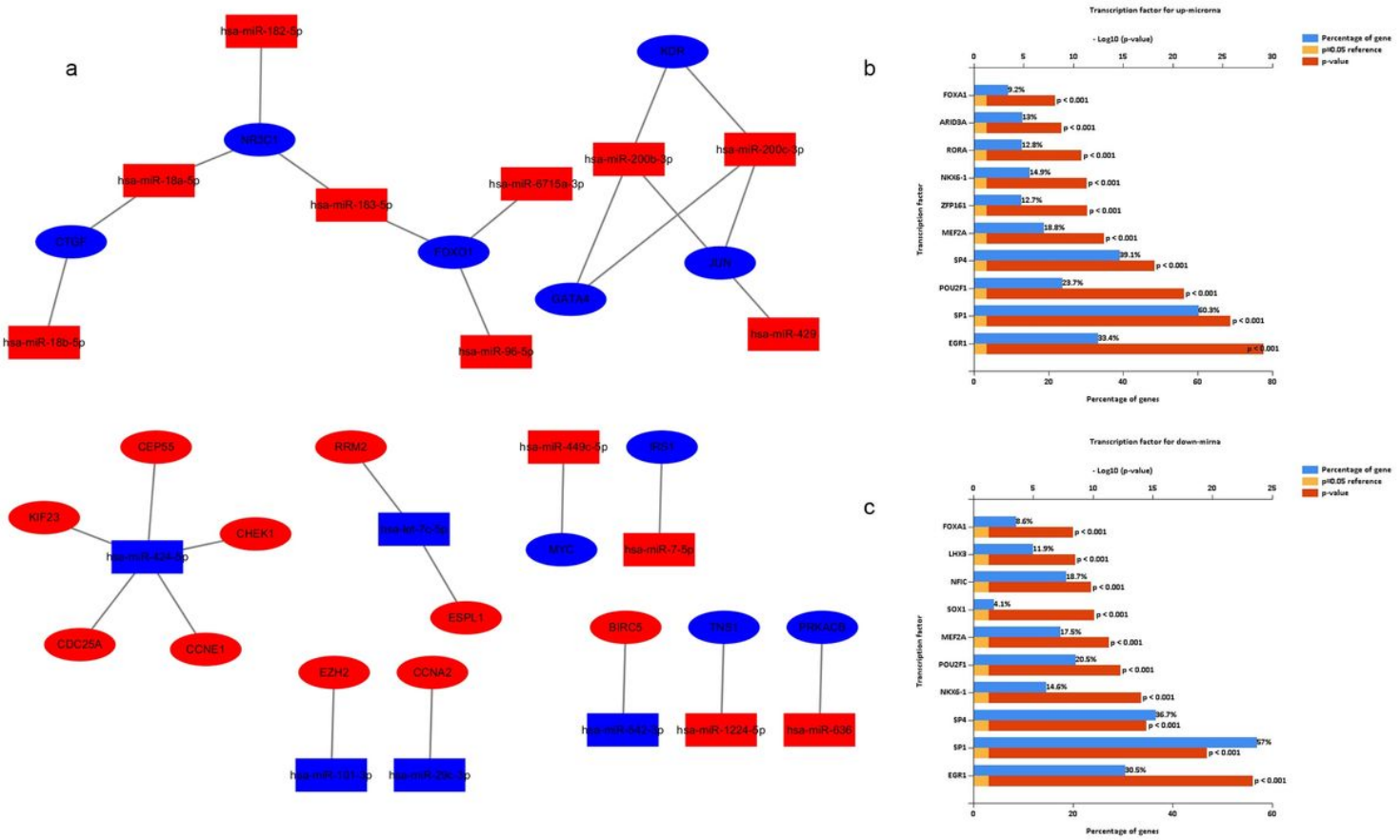


## Figure 12

Regulatory network of miRNA-mRNAs and corresponding transcription factors. (a)Regulatory network of RC associated genes and their target miRNAs. miRNAs: microRNA; Red represents upregulation. Blue represents downregulation. The oval represents mRNA. The rectangle represents miRNA. (b) Predicted transcription factors of upregulated DE-miRNAs; (c) transcription factors of downregulated DE-miRNAs.

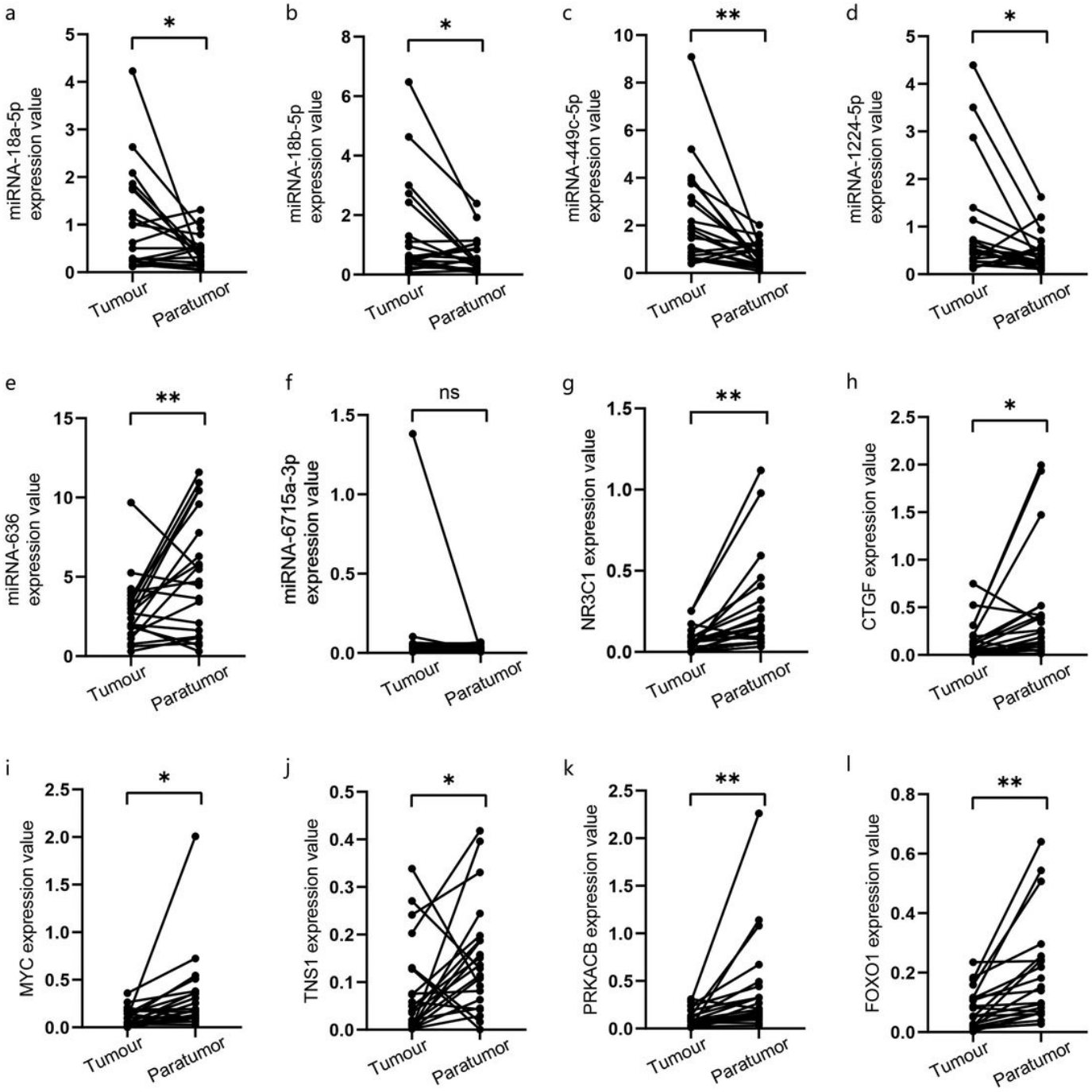


## Figure 14

Expression of potential miRNAs and target genes in EC tissues and normal adjacent tissues. (a-f) miRNA expression levels (g-l) mRNA expression levels. *p<0.05. **p<0.01.

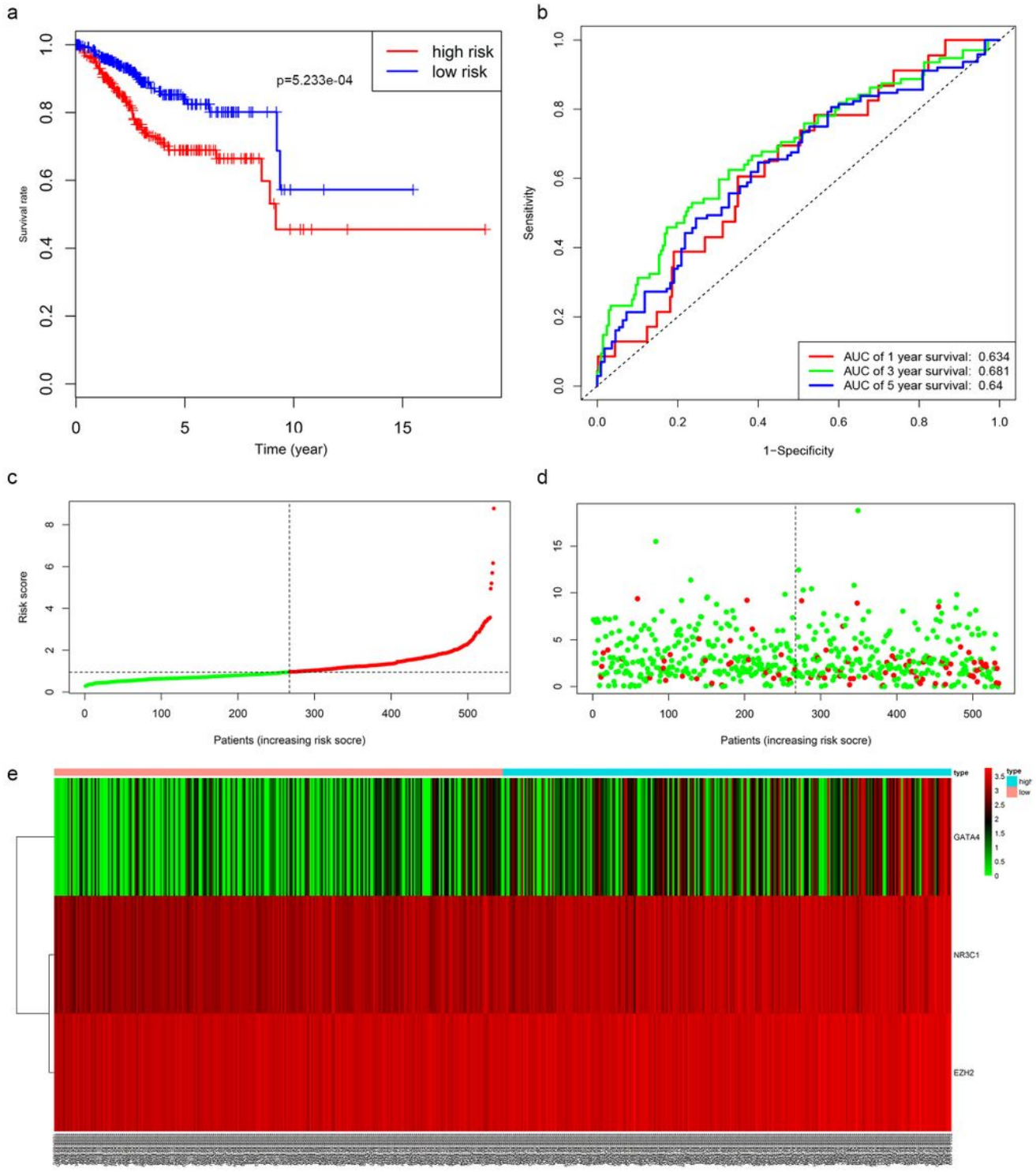


## Figure 16

Analysis of the prognostic model between low- and high-risk groups. (a) Kapla-Meier survival curve of overall survival between the high-risk group and low-risk group; (b) The time-dependent survival ROC curves; (c) The distributions of risk score; (d) Survival status; (e) The heatmap shows the expression levels of the three genes in low- and high-risk groups.

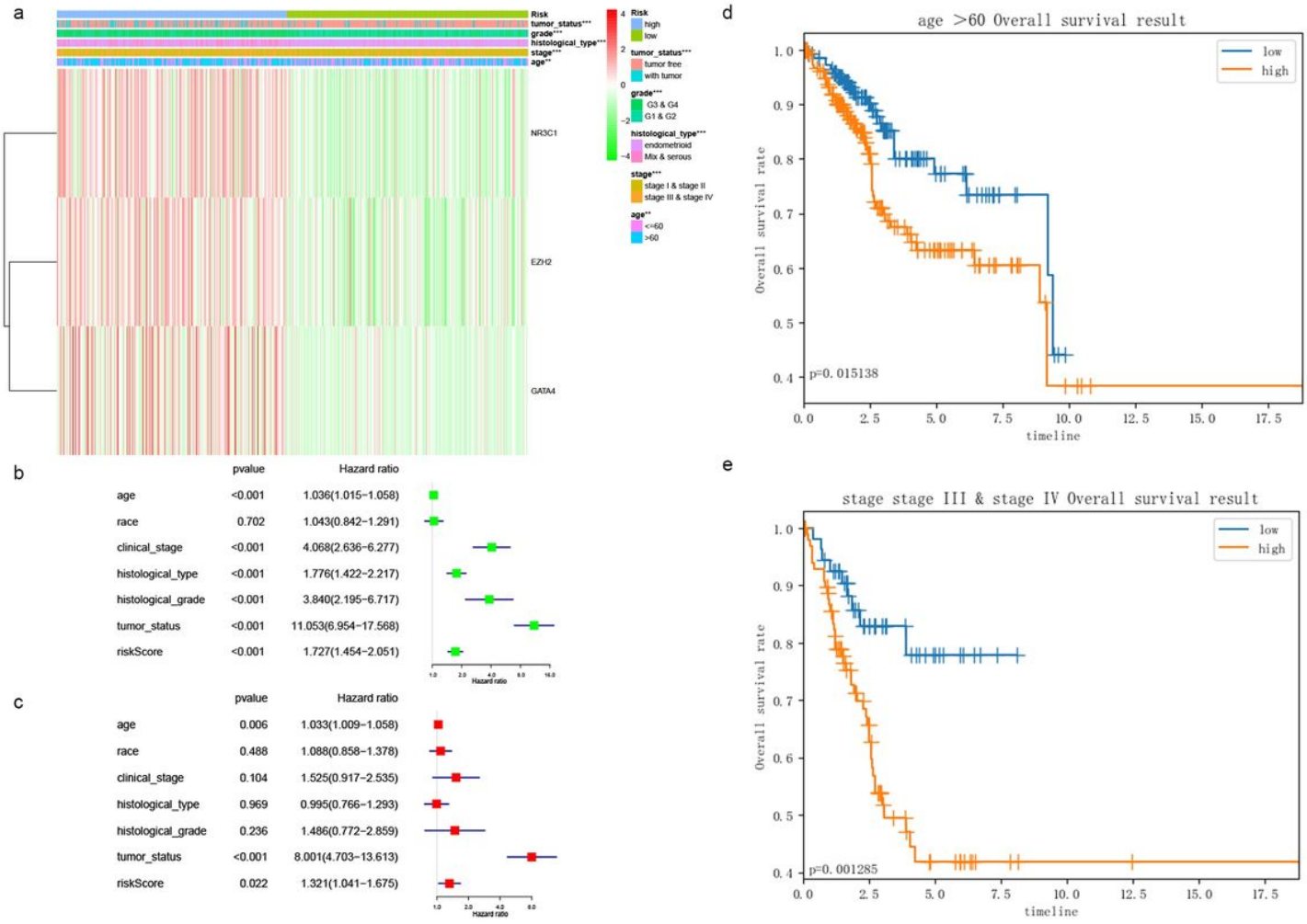


## Figure 18

Study of the factors impacting prognosis of EC. (a) The heatmap shows the distribution of clinicopathological features was compared between the low- and high-risk groups. ** p<0.01; *** p<0.001. (b) Forest Plot for univariate Cox regression analysis of clinical factors and risk score. (c) Forest Plot for multivariate Cox regression analysis of clinical factors and risk score. (d) Kaplan-Meier survival curve of age ≥60 years old subgroup between the low- and high-risk groups for the overall survival rate in endometrial carcinoma. (e) Kaplan-Meier survival curve of stage III/IV subgroup between the low- and high-risk groups for the overall survival rate in endometrial carcinoma

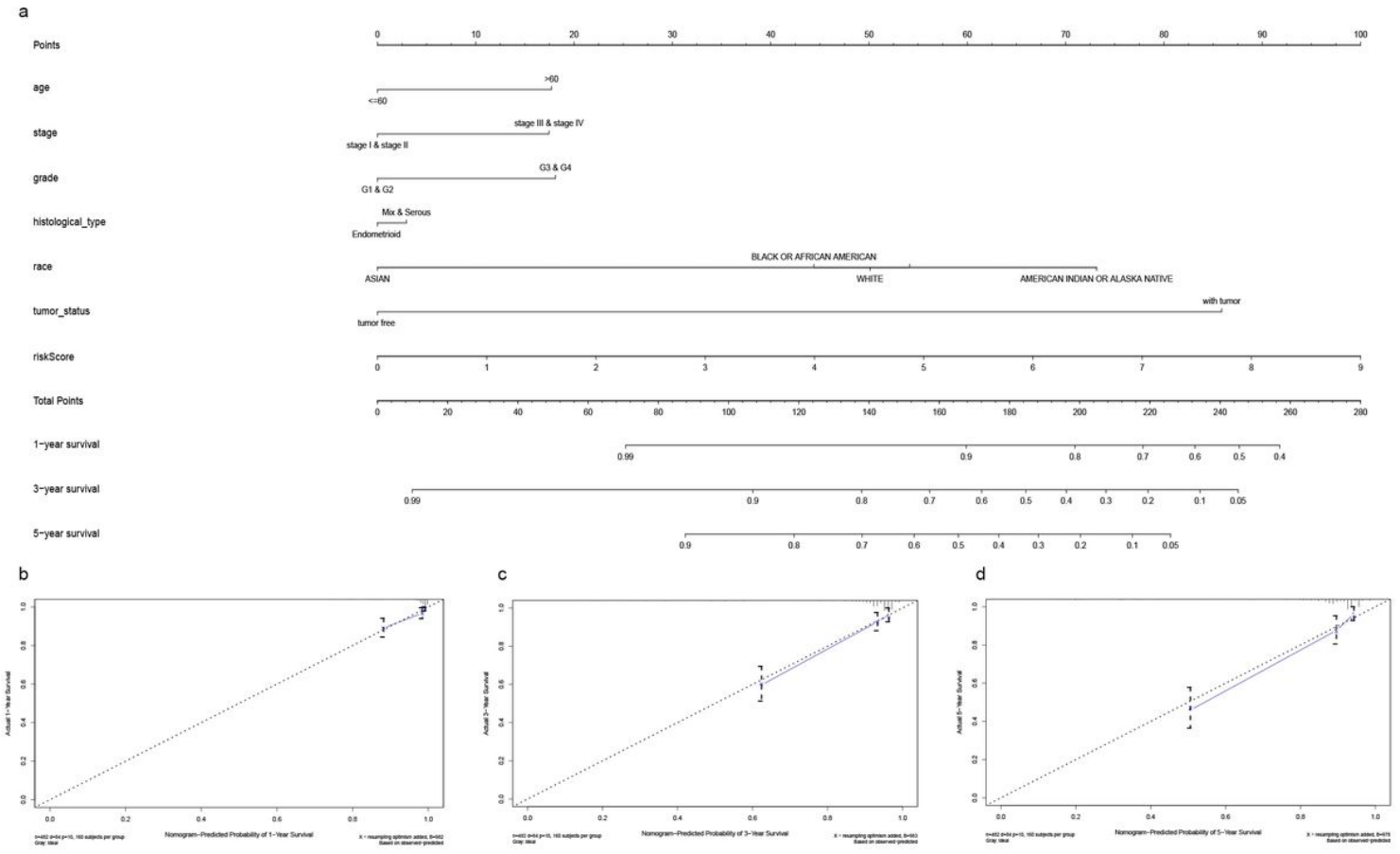


## Figure 20

Nomogram predicting overall survival for EC patients. (a) For each patient, 33 seven lines are drawn upward to determine the points received from the seven predictors in the nomogram. The sum of these points is located on the 'Points' axis. Then a line is drawn downward to determine the possibility of 1□, 3□, and 5□year overall survival of EC. (b) The calibration plot for internal validation of the nomogram. The Y□axis represents actual survival, and the X□axis represents nomogram□predicted survival.

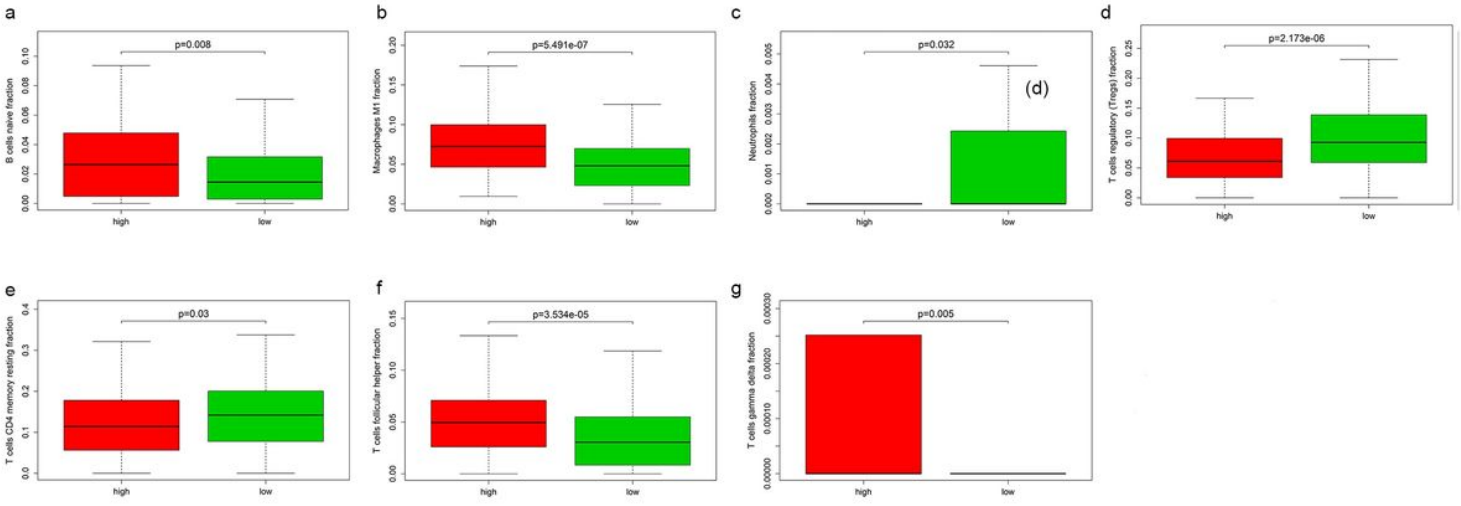


## Figure 21

The relationship of risk score with the significant immune cell. (a) B cells naive fraction. (b) Macrophages M1. (c) Neutrophils. (d) T cells regulatory (Tregs). (e) T cells CD4 memory resting. (f) T cells follicular helper. (g) T cells gamma delta.

## Supplementary Files

This is a list of supplementary files associated with this preprint. Click to download.

- SI.zip
- SI.zip